JGR Atmospheres

RESEARCH ARTICLE
10.1029/2020JD032798

ECTACI: European Climatology and Trend Atlas of Climate Indices (1979–2017)

D. Peña-Angulo[1], F. Reig-Gracia[1], F. Domínguez-Castro[2,3], J. Revuelto[1], E. Aguilar[4], G. van der Schrier[5], and S. M. Vicente-Serrano[1]

[1]Instituto Pirenaico de Ecología, Consejo Superior de Investigaciones Científicas, Zaragoza, Spain, [2]Aragonese Agency for Research and Development Researcher (ARAID), Zaragoza, Spain, [3]Department of Geography, University of Zaragoza, Zaragoza, Spain, [4]Center for Climate Change, Universitat Rovira i Virgili, Tarragona, Spain, [5]Royal Netherlands Meteorological Institute (KNMI), De Bilt, The Netherlands

Key Points:
- Four statistical parameters are obtained (climatology, coefficient of variation, slope, and significant trend) from 125 climate indices for the whole Europe
- The analysis of the seasonal trend of climate indices showed that there are large differences between seasons
- The data set and ECTACI map viewer are available for free (http://ECTACI.csic.es/)

Supporting Information:
- Supporting Information S1

Correspondence to:
D. Peña-Angulo,
dpa@ipe.csic.es

Citation:
Peña-Angulo, D., Reig-Gracia, F., Domínguez-Castro, F., Revuelto, J., Aguilar, E., van der Schrier, G., & Vicente-Serrano, S. M. (2020). ECTACI: European climatology and trend atlas of climate indices (1979–2017). *Journal of Geophysical Research: Atmospheres*, *125*, e2020JD032798. https://doi.org/10.1029/2020JD032798

Received 24 MAR 2020
Accepted 14 JUN 2020
Accepted article online 20 JUN 2020

Author Contributions:
Conceptualization: S. M. Vicente-Serrano
Data curation: J. Revuelto, E. Aguilar, G. van der Schrier, S. M. Vicente-Serrano
Formal analysis: D. Peña-Angulo, F. Reig-Gracia
Investigation: D. Peña-Angulo, F. Reig-Gracia, F. Domínguez-Castro, J. Revuelto, E. Aguilar, G. van der Schrier, S. M. Vicente-Serrano
Methodology: D. Peña-Angulo, F. Domínguez-Castro, S. M. Vicente-Serrano
Resources: J. Revuelto, E. Aguilar, G. van der Schrier, S. M. Vicente-Serrano
Software: F. Reig-Gracia, F. Domínguez-Castro
Supervision: J. Revuelto, E. Aguilar, G. van der Schrier, S. M. Vicente-Serrano
(continued)

Abstract A fundamental key to understanding climate change and its implications is the availability of databases with wide spatial coverage, over a long period of time, with constant updates and high spatial resolution. This study describes a newly gridded data set and its map viewer "European Climatology and Trend Atlas of Climate Indices" (ECTACI), which contains four statistical parameters (climatology, coefficient of variation, slope, and significant trend) from 125 standard climate indices for the whole Europe at 0.25° grid intervals from 1979 to 2017 at various temporal scales (monthly, seasonal, and annual). In addition, this study shows, for the first time, the general trends of a wide variety of updated standard climate indices at seasonal and annual scales for the whole of Europe, which could be a useful tool for climate analysis and its impact on different sectors and socioeconomic activities. The data set and ECTACI map viewer are available for free (http://ECTACI.csic.es/).

1. Introduction

Climate has a strong impact on different sectors of society, such as tourism (Amelung & Viner, 2006; Nicholls & Amelung, 2008), human health (IPCC, 2013; Woodward et al., 2014), agriculture (Fischer et al., 2005; Koufos et al., 2018; Moral et al., 2017; Piticar et al., 2018), and ecology (Easterling et al., 2000), among others. Furthermore, economic sectors largely dependent on weather conditions (agriculture, water resources, fisheries, tourism, etc.) are increasingly conditioned by the impacts from climate change (Hoegh-Guldberg et al., 2018). Extreme weather events cause economic loss, as well as to human lives, which together with a society that has become more vulnerable point to the urgent need to increase our knowledge on climate change (Easterling et al., 2000) and for climate information.

Researchers, policy makers, and the general public are demanding climate services that are more readily applicable to specific areas of society. However, some sectors such as tourism, energy, and agriculture demand tailored information that is not usually directly available. For example, some sectors are affected by the combination of meteorological variables; for example, the combination of temperature, relative humidity, and solar radiation is important for the human comfort index, which is used in public health monitoring (Di Napoli et al., 2018; Goldie et al., 2019). However, other sectors need information on mean values in a specific period of the year, for example, agriculture during the growing season. To meet these demands, a huge amount of specific climate indices have been created from raw climate variables (Easterling et al., 2003; Yu et al., 2009).

Climate indices are important indicators of the state and changes in the climate system (Williams & Eggieston, 2017). Each climate index is based on certain parameters and describes statistical characteristics defining a time series of climate variables, such as its mean, extreme, or trend. Over the past decades, several studies have analyzed changes in climate indices in various regions and periods. WorldClim (Hijmans et al., 2005) global space coverage is a set of global climate layers containing average monthly gridded climate data for the period 1970–2000 at different spatial resolutions. This data set includes the minimum, mean, and maximum temperature, precipitation, and derived bioclimatic indices. Alexander et al. (2006) also used global space coverage to make a study on the changes in daily climate extremes of temperature and precipitation for different periods. In Europe, studies have analyzed changes in climate indices. The joint CCl/CLIVAR/JCOMM Expert Team (ET) on Climate Change Detection and Indices (ETCCDI)

Validation: D. Peña-Angulo, F. Reig-Gracia, F. Domínguez-Castro
Visualization: J. Revuelto, E. Aguilar, G. van der Schrier, S. M. Vicente-Serrano
Writing - original draft: D. Peña-Angulo
Writing – review & editing: D. Peña-Angulo, F. Reig-Gracia, F. Domínguez-Castro, J. Revuelto, E. Aguilar, G. van der Schrier, S. M. Vicente-Serrano

developed a suite of climate change indices primarily focusing on extremes (Alexander et al., 2006; Frich et al., 2002; Klein Tank & Können, 2003; Klein Tank et al., 2009) and developed software to calculate climate indices. The core set of 27 extreme indices developed by ETCCDI is commonly used in climate studies worldwide, for example, China (Hong & Ying, 2018), India (Panda et al., 2016), and Europe (Van den Besselaar et al., 2013).

On the other hand, the EMULATE project (European and North Atlantic daily to MULtidecadal climate variability) carried out systematic mapping of the trend observed in 64 temperature and precipitation indices based on daily instrumental records for the period 1901–2000 (Moberg et al., 2006); however, access is limited (Chen et al., 2015). Additionally, Klein Tank and Können (2003) examined trends in the six indices for daily temperature and seven indices for precipitation extremes for the period 1946–1999 from more than 100 stations in Europe. This study found symmetric warming of the cold and warm tails on the distribution of daily minimum and maximum temperatures for several periods: from 1946 to 1975, slight cooling occurred, and from 1976 to 1999, warming became more apparent, and the number of wet days increased. The same study also indicated the need to carry out research using a higher density of weather stations. Several studies on the trend of climate indices have also been carried out on a national level, for example, China (Yin et al., 2015), the western Indian Ocean (Vincent et al., 2011), the United States (Heim, 2015), southwestern Spain (Moral et al., 2017), Turkey (Toros, 2012), and Cyprus (Katsanos et al., 2018), among others. General conclusions and questions emerge from these findings: (i) the low density of weather stations and especially their irregular spatial distribution has not prevented a comprehensive picture of the climate indices from being obtained; (ii) most studies focus on temperature and precipitation indices, with very few involving other types of climate indices; (iii) most studies focus on climatic indices that evaluate extreme events.

This paper aims to provide a comprehensive analysis of the climatology and recent temporal evolution of seasonal and annual values from 117 climate indices covering the whole of Europe in the period 1979–2017. Following an exhaustive literature review, these were deemed the most important ones for the priority sectors of the Global Framework for Climate Services, that is, agriculture, disaster risk reduction, energy, health, water, and tourism. This was the first time a wide variety of climate indices for the whole of Europe had been used and estimated with updated data and high spatial resolution. The main objectives were (i) to generate a spatial climatology from the indices in order to understand climate characteristics beyond the climatology of average values and (ii) to find changes in these indices over the last four decades at seasonal and annual scales. Furthermore, this study presents a new gridded data set and map viewer (ECTACI: European Climatology and Trend Atlas of Climate Indices) showing monthly, seasonal, and annual climatology, coefficient of variation, and trend from 125 climate indices in Europe (1979–2017).

2. Data and Methods

2.1. Climate Indices

This study uses the "ClimInd" package within the R platform (https://cran.r-project.org/web/packages/ClimInd/index.html) to compute 125 climate indices at monthly, seasonal, and annual temporal frequency for Europe (125 at monthly scale and 117 at seasonal and annual scales). The specific definition for each index can be seen in Figure 1, and details of the climate index data set can be found in Domínguez-Castro et al. (2020). The 125 climate indices were selected from a review of the literature (Alexander et al., 2006; Frich et al., 2002; Klein Tank & Können, 2003; among others) and their impact on the high-priority sectors (agriculture, disaster risk reduction, energy, health, water, and tourism) and grouped into eight categories: temperature (42), precipitation (21), bioclimatic (21), aridity/continentality (10), cloud/radiation (5), wind (6), snow (12), and drought (8).

A gridded database of the 125 climate indices was generated from the European Climate Assessment and Dataset (ECA&D) E-OBS-gridded data set v17.0 (Cornes et al., 2018) and the ERA5 reanalysis database (Copernicus Climate Change Service, 2017). The ECA&D contains quality-controlled meteorological records, sourced from the European National Meteorological Services, and the E-OBS is the gridded data set based on the information from these stations. The ERA5 is the latest generation of the reanalysis data set developed by the European Center for Medium-Range Weather Forecasts (EWMF). We used ERA5 data to obtain the climate variables not found in the observational data set. In spite of the different characteristics of both databases, we unified the criteria of the two to work with the same spatial cover (0.25°, 12,280 time

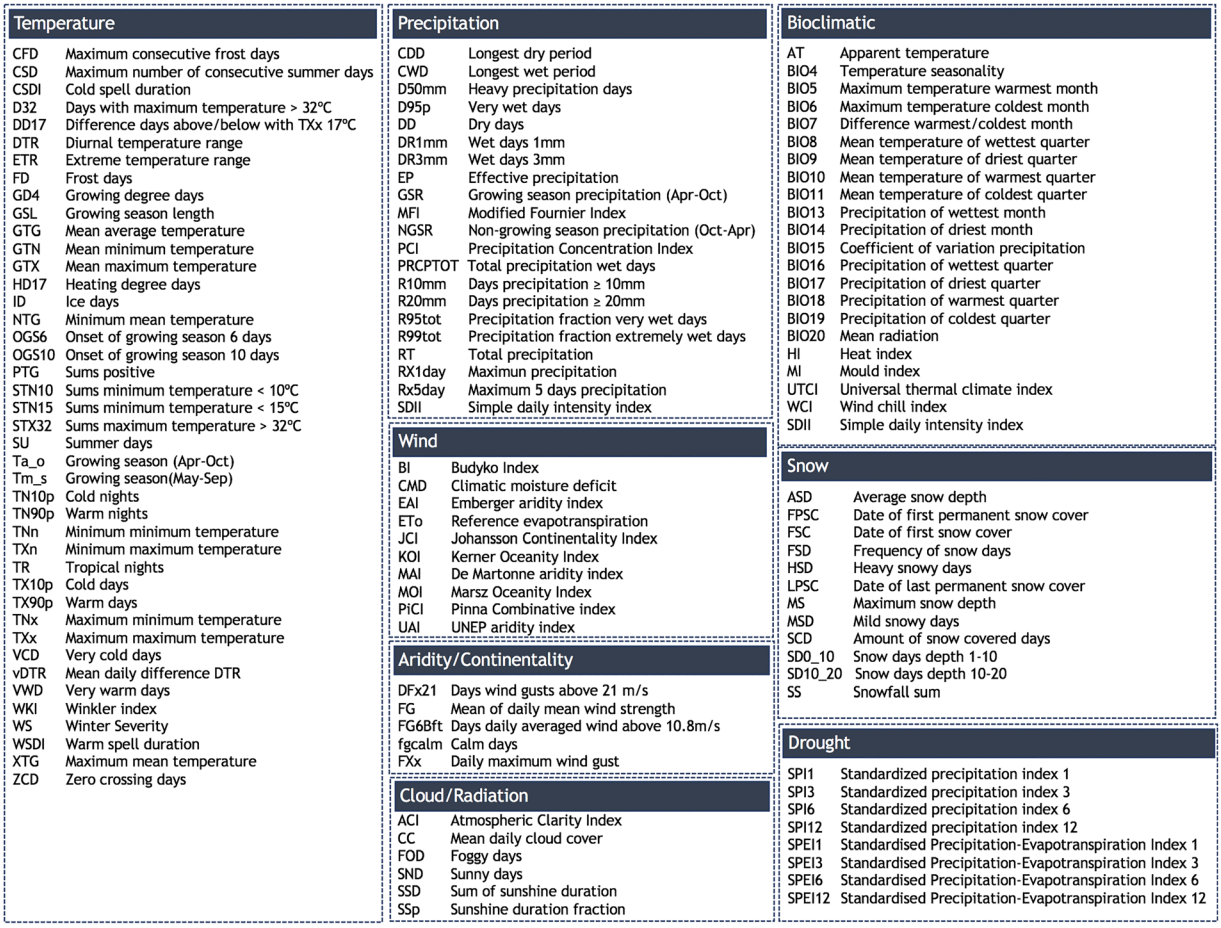

Figure 1. Climate indices (abbreviation and definition) used in this study.

series), temporal (monthly, seasonal, and annual), and period (1979–2017) throughout Europe. In some cases, the climate index was calculated only on annual scale. Indices requiring a base period for their calculation took the entire period as a reference (i.e., TX10p, TX10p, CDD, VCD, VWD, TX90p, TN90p, WSDI, R95tot, R99tot, and D95p).

2.2. Statistical Analysis

The study obtained four statistics for each climatic index and for 12,280 series covering Europe at monthly, seasonal, and annual scales for the whole period (1979–2017): (1) mean climatology, (2) coefficient of variation in order to find the interannual variability, (3) slope of the linear model in order to find the magnitude of change, and (4) trend significance by means of the Mann-Kendall test. The linear trend was estimated by the ordinary least squares method; which is widely used in climate studies (Kiktev et al., 2003; Moberg & Jones, 2005; Moberg et al., 2006). The trend significance at levels of $p < 0.05$ and $p < 0.01$ was evaluated with the Mann-Kendall test taking into account serial correlation (Alexander et al., 2006; Kiktev et al., 2003). Positive/negative signals are expressed by colors (red/blue), and the significance in the Mann-Kendall test is shown by three color variations, not significant, significant at p level < 0.05 and significant at p level < 0.01. The ECTACI data set and map viewer contain the spatial distribution of the four statistics: climatology, coefficient of variation, slope, and significant trend. The statistical analyses applied to the 125 climate indices were checked for consistency in their spatial distribution from map viewer.

For the first time, many of the climate indices were included in the same spatial and study period at different temporal scales. Consult Figure 1 when analyzing the results and discussion section of this study, which includes abbreviations, names, and temporal scales of the climate indices. In the results section, the

climatology and trend of the 117 indices at seasonal and annual scales are shown by percentage of land with positive and negative trends in all indices and spatial distribution of statistics of those selected which are a good example of the rest of the indices of each category (temperature, FD and GTG; precipitation, RT; aridity/continentality, CDM; cloud/radiation, CC and SSp; wind, FXx; and snow, FSD; see Figure 1 for abbreviations used). The selected climate indices belong to each category in the study and represent an example of the behavior of the other indices according to their category. Furthermore, it presents a new gridded data set and map viewer (ECTACI) showing the monthly, seasonal, and annual climatology, coefficient of variation, and trend of the 125 climate indices in Europe (1979–2017).

All statistical procedures, maps, and plots used the R statistical programming language (R Core Team and R Development Team Core, 2017), packages "ClimInd" climatic indices; ncdf4 for NetCDF format; maptools, maps, rgeos, raster, and rgdal for spatial data manipulation; and ggplot2 for mapping and plotting.

3. Results

3.1. Annual and Seasonal Trends of Climate Indices Throughout Europe

3.1.1. Climatology of Climate Indices Throughout Europe

The spatial climatology of selected climate indices across the Europe is shown in Figure 2 through reporting statistical parameters (mean and coefficient of variation) for each grid cell of the ECTACI data set at annual scales from 1979 to 2017. Maximum values from FD index climatology (Figure 2a) were recorded over northern Europe (Norway, Sweden, Finland, and Iceland) and mountain areas (Alps, Carpathians, and Pyrenees), while minimum values were recorded in southern Europe, especially in the Mediterranean area. The climatology of GTG (Figure 2b) and SSP (Figure 2f) indices has a strong latitudinal component, with maximum values in the south and minimum values in the north of the study area. The opposite is true of the CC index (Figure 2e), which has maximum values in the north and minimum values in the south. The maximum climatology from the RT index (Figure 2c) was measured in the northwest of the Scandinavian Peninsula, British Isles, Iberian Peninsula, and the Alps. CMD index maximum values (Figure 2d) were recorded in the south of the Iberian Peninsula. On the other hand, the FXx index (Figure 2g) showed a west-east spatial pattern, with maximum values in the west and minimum values in the east. The maximum FSD index climatology (Figure 2h) was measured in the Scandinavian Peninsula, Iceland, and mountain areas, while minimum values were found in southwest Europe, especially in the Iberian Peninsula. Lastly, the spatial variability of the selected climate indices is illustrated by the coefficient of variation (Figure 2).

3.1.2. Spatiotemporal Annual Trends of Climate Indices Throughout Europe

In general, the spatial variability of the trend in annual climate indices is important. Spatial behavior can be summarized into three categories: (i) climate indices with a high percentage of land (more than 75%) with a positive trend, (ii) climate indices with a high percentage of land (more than 75%) with a negative trend, and (iii) climate indices that do not show a clear positive or negative trend (more than 25% and less than 75% of the land). The trend in annual climate indices can be observed in Figure 3, which depicts the percentage of land with positive or negative trends, significant (p level < 0.05) or not significant (p level > 0.05) of the 117 climate indices at annual scale in Europe. Following the order of the previously defined categories, the climate indices showing more than 75% of land with a positive trend are for temperature (CSD, DD17, GD4, GSL, GTG, GTN, GTX, NTG, TNn, TXn, PTG, SU, Ta_o, Tm_s, TN90P, TX90P, VWD, WKI, WS, WSDI, XTG, TNx, and TXx), for aridity/continentality (ETo), and for cloud/radiation (ACI, SND, SSD, and SSp). On the other hand, the climate indices with a negative trend in more than 75% of land are for temperature (CFD, CSDI, FD, HD17, ID, OGS10, OGS6, STN10, STN15, TN10P, TX10P, and VCD), for aridity/continentality (KOI), for cloud/radiation (CC and FOD), and for snow (ASD, FSD, LPSC, MS, SCD, SD0_10, and SS). Finally, climate indices that do not show a clear positive or negative trend (more than 25% and less than 75% of land) are for temperature (DTR, ETR, vDTR, and ZCD), for wind (DFX21, FG, FG6BFT, fgcalm, and FXx), and for snow (FPSC and FSC). The major part of the precipitation and aridity/continentality indices are characterized by a very diverse trend throughout space. The snow indices HSD and SD10-20 do not have a clear spatial representation of the trend (less than 25% of land with positive and negative trends).

From the previous results, general patterns in the annual trend of categories in the study could be extracted, summarized in Figure 4. The temperature indices were divided between those with a negative trend and indicated cold days and nights, such as the FD index (Figure 4a), while other indices showed a positive

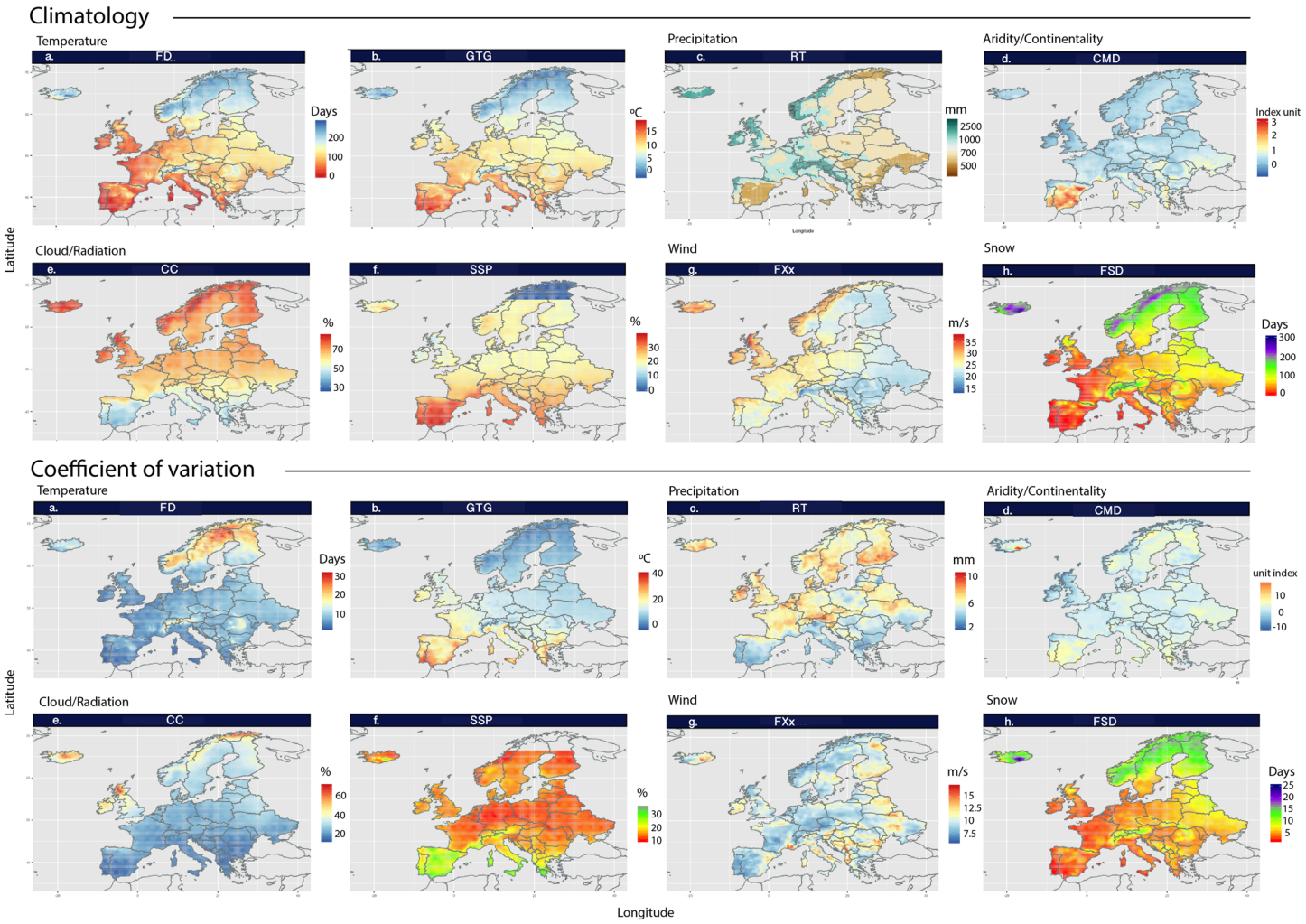

Figure 2. Annual spatial distribution of the climatology and variability of eight climate indices for Europe in the period 1979–2017. Each index belongs to one of six categories: temperature, (a) FD and (b) GTG; precipitation, (c) RT; aridity/continentality, (d) CMD; cloud/radiation, (e) CC and (f) SSP; wind, (g) FXx; and snow, (h) FSD.

trend and indicate warm days and nights, such as the GTG index (Figure 4b). Most precipitation indices had a large spatial variety in their trend, for example, RRT (Figure 4c). The indices included in the bioclimatic category were divided between the ones with trends very similar to those of temperatures and those that are similar to precipitation. The aridity/continentality indices showed spatial differences in their trends, for example, CMD (Figure 4d). On the contrary, indices included in the cloud/radiation category differed between those reflecting the characteristics of the cloudiness with a negative trend, for example, CC (Figure 4e), and those reflecting the characteristics of the radiation with a positive trend, for example, SSP (Figure 4f). The indices in the wind category did not generally show a clear trend, but were sometimes negative, for example, FXx (Figure 4g). Finally, the indices included in the snow category showed a negative trend, with the exception of the very coldest areas in Europe, for example, FSD (Figure 4h).

In the trend analysis, in addition to obtaining the sign and significance of the trend, we analyzed the magnitude of change. Figure 5 shows the spatial distribution of the magnitude of trend in each selected climate index. The major decrease in the FD index (Figure 5a) was located in the inland areas of Europe, while a strong increase in the GTG index (Figure 5b) occurred in the same area. On the other hand, a clear decrease in the RT index (Figure 5c) was observed in France and its surroundings. The CMD index (Figure 5d) showed spatial differences in their trends, with the largest increase in the south and the largest decrease in the north of the study area. The CC (Figure 5e) and SSP (Figure 5f) indices had an opposite trend, with

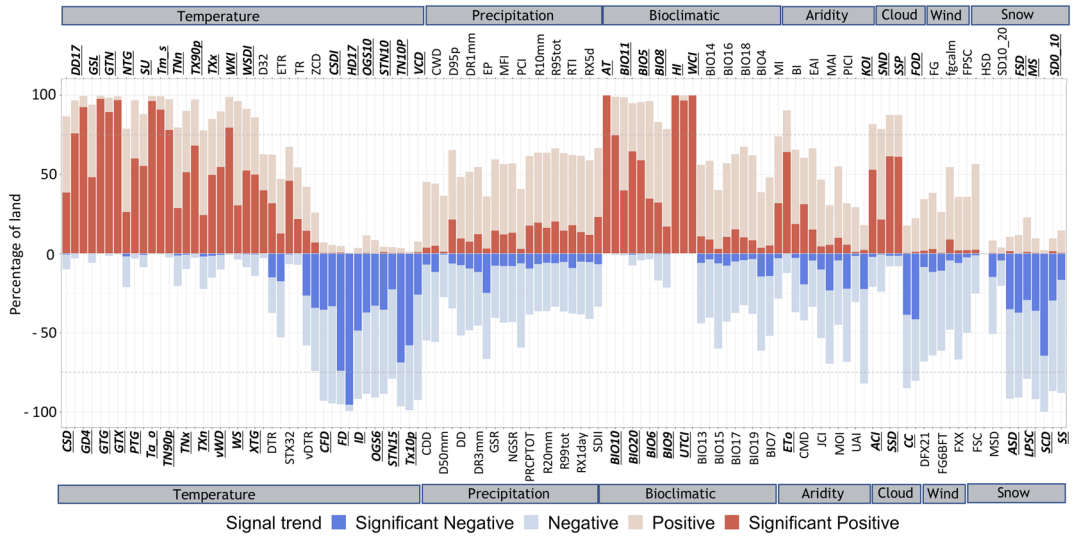

Figure 3. Percentage of land with a positive or negative trend, significant (p level < 0.05) or nonsignificant (p level > 0.05) of the 117 climate indices at annual scale in Europe. The bold, underlined, and italic indices indicate more than 75% of land with positive or negative trend.

the largest decrease in trend found in the CC index and the largest increase in trend in the SSp index corresponding to inland areas of Europe. The FXx index (Figure 5g) showed great spatial variability, with a high increase in some areas, such as the Scandinavian Peninsula, and other areas with a decrease, for example, Ireland. Finally, the maximum decrease in the FSD index (Figure 5h) was observed in the Scandinavian Peninsula, Iceland, British Islands, and the inland areas of Europe.

3.1.3. Spatiotemporal Seasonal Trends of Climate Indices Throughout Europe

In addition to the differences observed in the trends of the defined categories, spatial and seasonal differences could also be found. The spatial differences seen in the trends are complex to analyze since there is

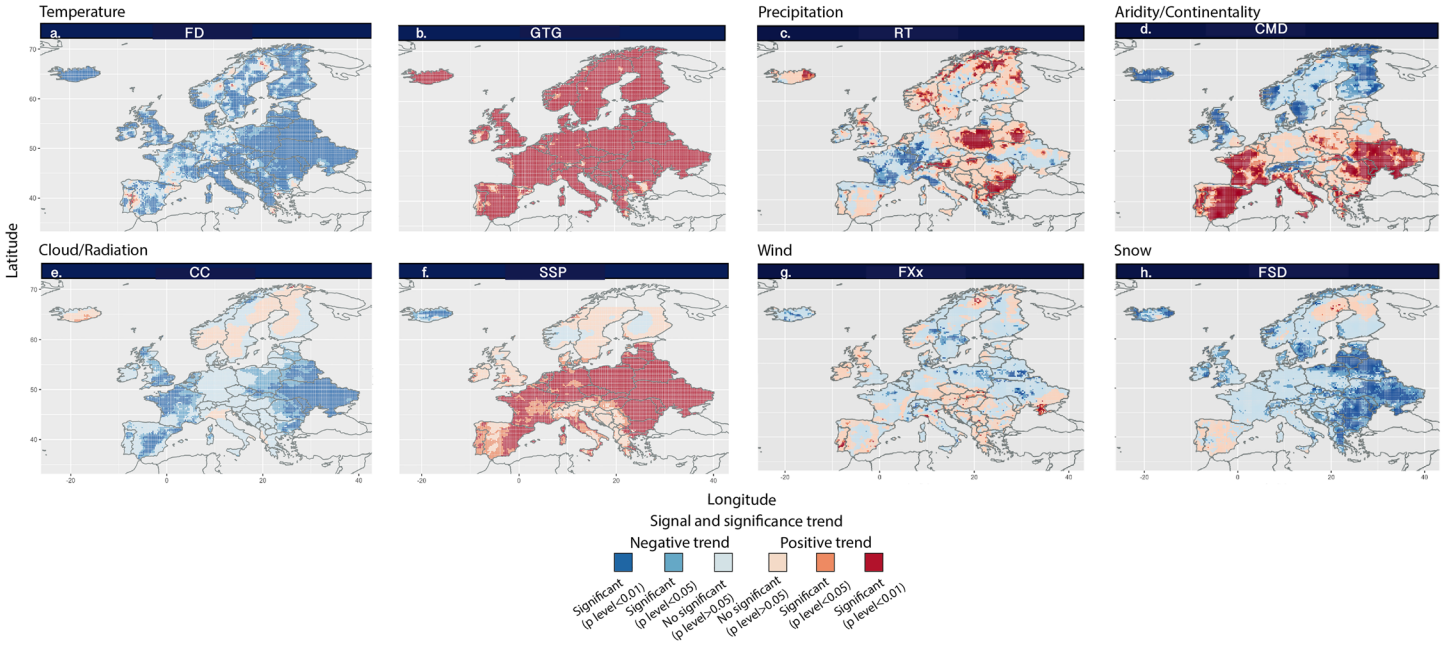

Figure 4. Spatial distribution of the trend of eight climate indices. Each index belongs to one of six categories: temperature, (a) FD and (b) GTG; precipitation, (c) RT; aridity/continentality, (d) CMD; cloud/radiation, (e) CC and (f) SSP; wind, (g) FXx; and snow, (h) FSD at the annual scale for Europe (1979–2017). The positive/negative signal is shown in color (red/blue), and the significance from the Mann-Kendall test is given in three colors variations, nonsignificant, significant at p level < 0.05 and significant at p level < 0.01.

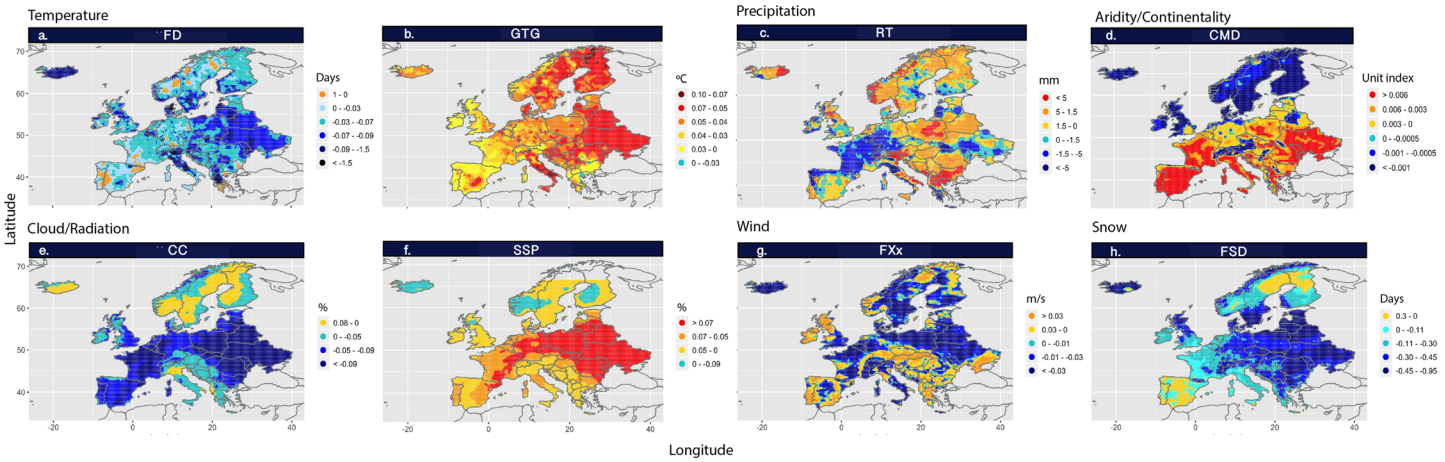

Figure 5. Spatial distribution of the magnitude of the trend of eight climate indices at annual scale for Europe (1979–2017). Each index belongs to one of six categories: temperature, FD and GTG; precipitation, RT; aridity/continentality, CMD; cloud/radiation, CC and SSP; wind, FXx; snow, FSD.

no continuous pattern, due to several causes, such as orography, areas distant from the sea and latitude, among others. There were different patterns in the seasonal trend of the climate indices selected for the period and study area, which are summarized in Figure 6 and Table S1 in the supporting information.

Figure 6 contains the percentage of land with a significant trend in more than 25% of the land in all season. The temperature indices with a significant trend in more than 25% of the land in all seasons but having a positive signal are GTG, GTN, GTX, TNn, and TN90p, while those with negative signal are HD17 and TN10p. On the other hand, the temperature indices with a significant trend in more than 25% of the land

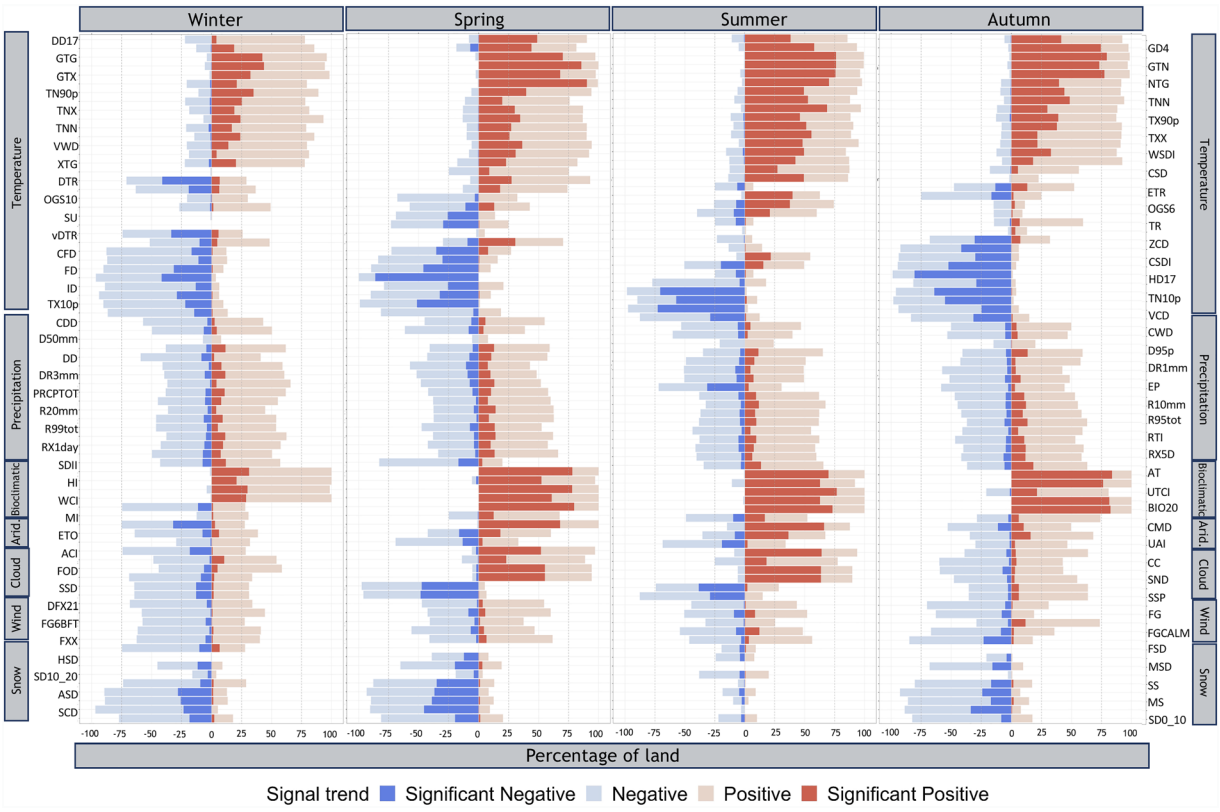

Figure 6. Percentage of land with a significant (p level < 0.05) positive or negative trend of the 117 climate indices in winter, spring, summer, and autumn in Europe.

in spring and summer and, occasionally, also in autumn with a positive signal are NTG, TXn, TX90p, TNx, XTG, and TXx, while a negative signal is found in TX10p. There are some temperature indices with positive and negative trends in different seasons, for example, DTR with a negative trend in winter and a positive trend in spring and summer and vDTR with a negative trend in autumn and winter and a positive trend in spring. Lastly, the WSDI index has a positive trend in summer and autumn, and VCD has a negative trend in summer. The temperature indices based on a threshold (e.g., FD, CFD, GD4, DD17, OGS6, OGS10, ID, and ZCD) are not included in this section because it is not possible to make a seasonal comparison.

For precipitation indices, the trend is only significant in more than 25% of the land in the EP index, with a negative trend in summer. Moreover, the aridity/continentality indices do not have a clear significant trend throughout the study area; only the ETo index has a positive trend in spring and summer, and CMD has a negative trend in winter and positive trend in summer. In all case, the cloud/radiation indices show a clear significant trend in spring and summer with a positive signal in the SSD, SSP, and ACI indices, and negative signal in CC and FOD. The wind indices do not show a significant trend. Finally, the snow category has a significant negative trend in winter, spring, and autumn in the ASD and MS indices, while this changes to the FSD and SCD indices in spring and the SCD index in autumn. Most climate indices show that the seasons with the largest changes in their signal trends are summer, followed by spring and autumn, while winter returns the lowest percentage of land affected by changes in trends.

Figure 7 shows the spatial distribution of the seasonal trends of the eight indices selected, ordered by categories. In the temperature category, the FD index shows a significant negative trend in most of the territory in winter, spring, and autumn (Figure 7a), while the GTG index has a significant positive trend for the whole of Europe in spring, summer, and autumn (Figure 7b). In precipitation category, RT does not show a clear significant trend (Figure 7c). For aridity/continentality, CMD has two spatial patterns, a significant positive trend in south and a significant negative trend in north of the study area, especially in spring and summer (Figure 7d). Cloud/radiation shows a significant negative trend in the CC index (Figure 7e) and a positive trend in SSP (Figure 7f) in spring and summer across most of the territory. In the wind category, the FXx index does not show a clear significant trend (Figure 7g). Finally, there is a negative trend in the FSD index in winter, spring, and autumn in the snow category (Figure 7h).

3.2. Features of the ECTACI Data Set and Map Viewer

The climatology, coefficient of variation, slope, and trend significance statistics of 125 climate indices at monthly, seasonal, and annual scales for Europe (1979–2017) are included in the ECTACI map viewer. This viewer is structured on different levels (Figure 8): the first level corresponds to the eight categories (temperature, precipitation, bioclimatic, aridity/continentality, cloud/radiation, wind, and snow), the second to the climatic index in each category, the third to the four statistics (climatology, coefficient of variation, slope, and significant trend), and the fourth level to the temporal scale (monthly, seasonal, and annual).

The monthly scale can be selected from 1 January to 12 December, while the seasonal scale ranges from 1 (winter: DJF) to 4 (autumn: SON). The ECTACI viewer includes basic information on the climate index (ID, name, description, importance, and time scale). Furthermore, the viewer can display the exact value of each statistic together with the graphic representation used by the legend (Figure 9). All information available in the ECTACI map viewer can be downloaded in 3-D NetCDF 4 format, available on the website http://ECTACI.csic.es/, maintained by the Spanish National Research Council. Each file download has an array of longitudes (464) × latitudes (201) × time (39 annual scales, 156 seasonal scales, and 468 monthly scales) for the period 1979–2017.

4. Discussion

4.1. Spatiotemporal Annual Trends of Climate Indices Throughout Europe

Assessing climate processes and impact is highly complex, since they are difficult to quantify and because of their subjectivity. In this context, the climate indices are useful tools in understanding the variability and impact of the climate on important sectors of society. Climate indices monitor the variations and changes in climate by examining different aspects of the raw variables; therefore, they usually help to inform users of the state of the climate. However, robust climate indices require databases built over the long term and

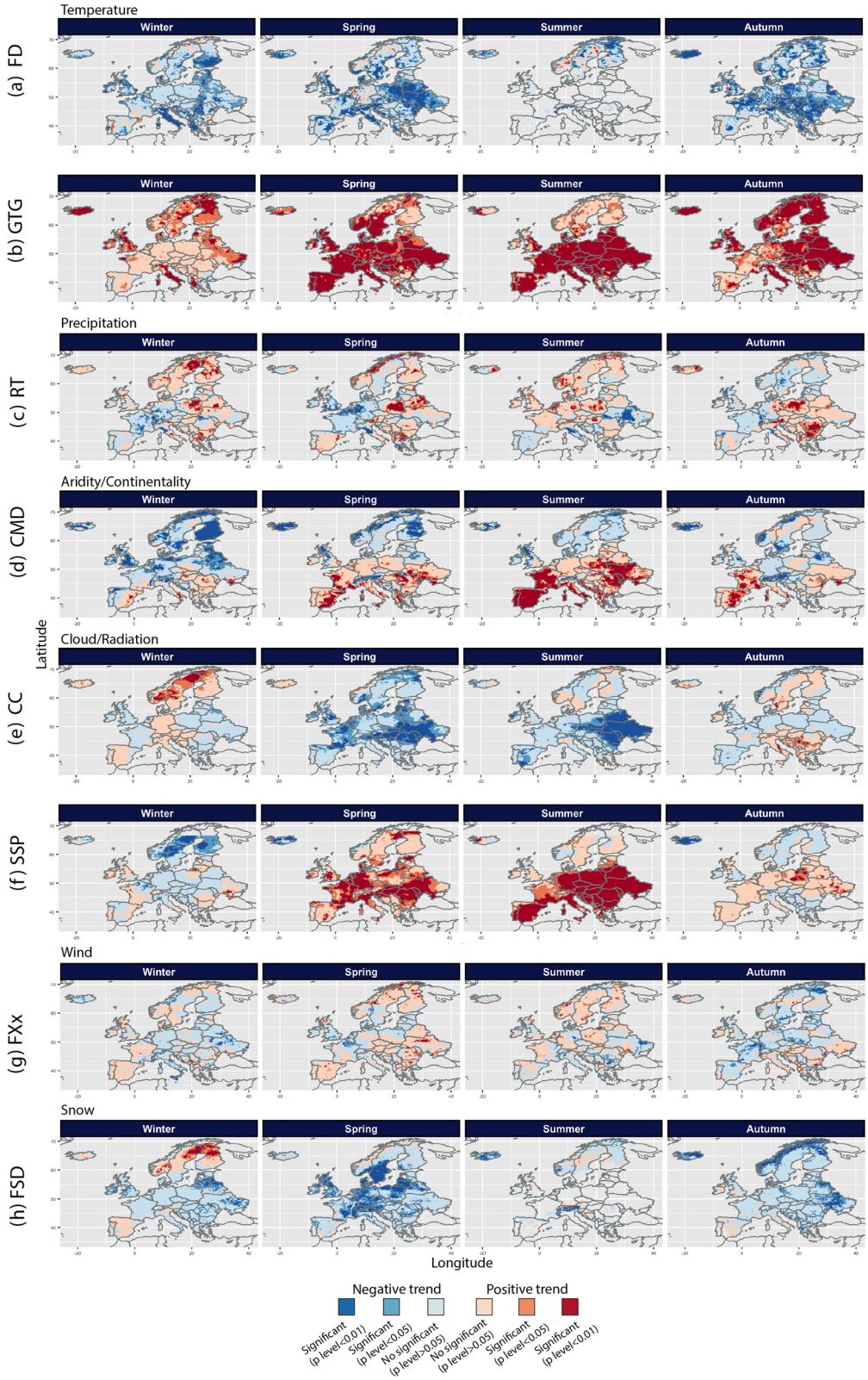

Figure 7. Spatial distribution of the trend of eight climate indices. Each index belongs to one of six categories: temperature, FD and GTG; precipitation, RT; aridity/continentality, CMD; cloud/radiation, CC and SSP; wind, FXx; snow, FSD at seasonal scale (winter, spring, summer, and autumn) for Europe (1979–2017). The positive/negative signal is shown in color (red/blue), and the significance from the Mann-Kendall test is given in three colors, nonsignificant, significant at p level < 0.05 and significant at p level < 0.01.

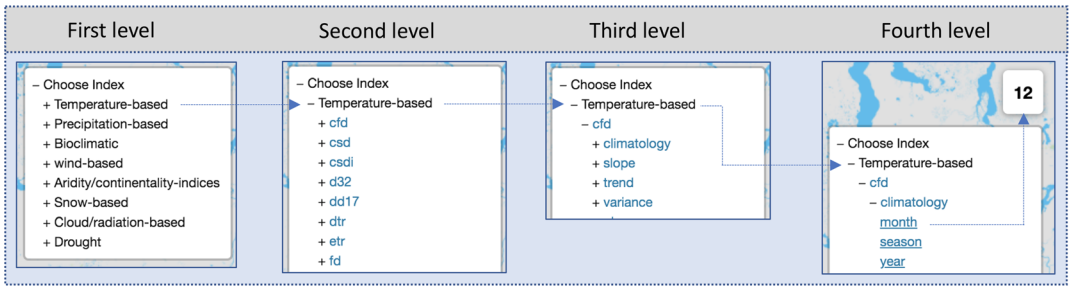

Figure 8. Structure level of the ECTACI map viewer.

characterized by high spatial resolution and extended spatial coverage so that they provide reliable information that is a true reflection of the dimension of climate change and its implications.

In this study, a special effort has been made to unify a large number of climate indices and analyze their temporal evolution throughout the study area (Figure 2). There are several studies on temperature and precipitation indices which quantify extremes (e.g., TN10p and TX90p), crossing thresholds (e.g., R10mm and R20mm), and the average (e.g., GTG, GTX, and GTN) (Alexander et al., 2006; Frich et al., 2002; IPCC, 2013; Klein Tank & Können, 2003; Moberg et al., 2006; Zhang et al., 2011). There are other less frequent climate indices that have heavy repercussions in certain sectors of society, such as agriculture, for example, GD4, OGS6, PTG, and GSR (Gabriels, 2006; Karl et al., 1999; Klein Tank et al., 2009; Martin-Vide, 2004; Winkler et al., 1974). Bioclimate indices are obtained from the WorldClim data set (Fick & Hijmans, 2017; Hijmans et al., 2005), which has been used extensively in agricultural, ecological, and hydrological assessments (Fick & Hijmans, 2017). There are other less frequent bioclimate indices which have importance in

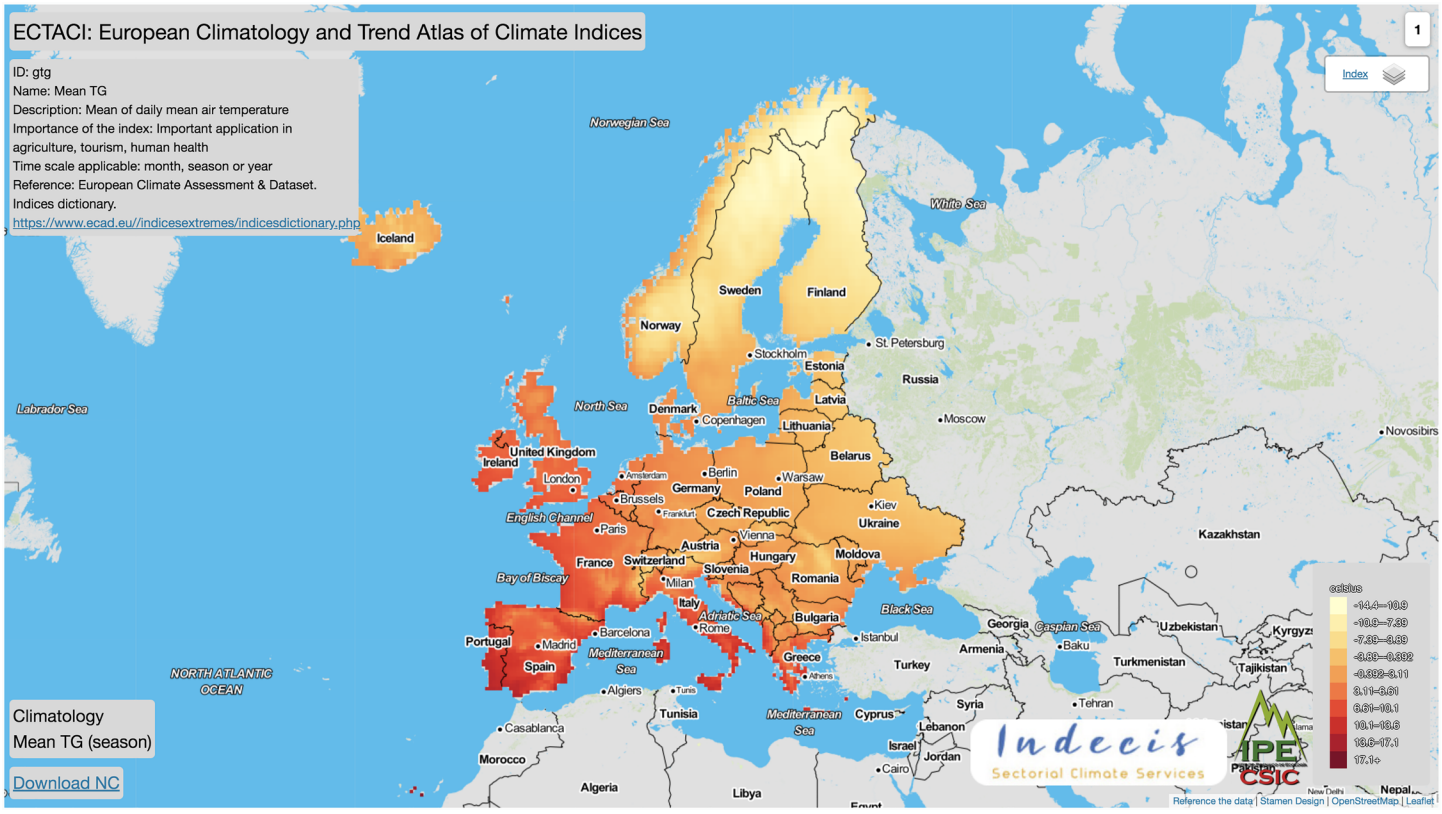

Figure 9. Web tool to visualize the statistics (climatology, coefficient of variation, slope, and significant trend) of the 125 standard climate indices in the ECTACI viewer and download the entire data set.

tourism and health sectors like UTCI, MI, HI, WCI, and AT (Bröde et al., 2012; Di Nappoli et al., 2018; Osczevski & Bluestein, 2005; Steadman, 1984).

The aridity/continentality indices are widely used in the ecology and agriculture sectors, due to the importance of plant-available water, for example, BI, JCI, KOI, PiCI, MAI, and MOI (Baltas, 2007; Creed et al., 2014). In addition, there are studies indicating that climate change will increase aridity globally as the rising temperatures drive up rates of evapotranspiration (Dai, 2011), so different aridity indices are applied, such as CMD, UAI, ETo, and EAI (Chiew et al., 1995; Girvetz & Zganjar, 2014; Huang et al., 2016; McGregor et al., 1988). Most studies on cloudiness and radiation use data from surface solar radiation or sunshine indices, for example, SSD, SSP, and CC (Sanchez-Lorenzo et al., 2008, 2015; Stjern et al., 2009; Wild, 2009).

In addition, the cloud/radiation indices are used to assess tourism and leisure facilities, for example, FOD and SND (Blazejczyk, 2006; Rudel et al., 2007). Wind energy is nonpolluting cost-effective and renewable, so wind indices, such as DFx21 and FG6Bft, are a valuable source of information (Azad et al., 2010). In addition, wind has substantial impact on society and the environment (human safety, maritime, and aviation activities, among others). For this reason, the FG and FXx indices are very useful in recognizing the temporal evolution of mean and maximum wind gust (Azorin-Molina et al., 2016).

On the other hand, the fgcalm index is valuable in studies on pollution in urban areas (Croxford et al., 1996). Finally, snow indices are widely used to assess the relationship between the winter tourism demand and snow depth, for example, ASD and MS (Falk, 2010; Pickering, 2011). Fontrodona Bach et al. (2018) indicated a decrease in maximum and mean snow depth over Europe, and this has strong implications for the availability of fresh water in spring.

This study has compiled the general trend from the wide variety of climate indices at seasonal and annual scales for Europe (1979–2017). In general, the results obtained are consistent with the review of the literature. The analysis of trends in temperature indices at annual scale showed general warming during the study period 1979–2017; the indices for cold days and night had a negative trend, while the warm days and nights showed a positive trend (Alexander et al., 2006; Frich et al., 2002; Klein Tank & Können, 2003; IPCC, 2013). Klein Tank and Können (2003) indicated positive trends in Europe for the indices of wet extremes from 1976 to 1999. Similarly, Frich et al. (2002) highlighted a significant increase in most heavy precipitation indicators for parts of Europe from 1946 to 1999. However, Alexander et al., 2006 found that the trend of precipitation indices had poor spatial coherence for the period 1951–2003. In this study, the majority of precipitation indices did not show a general trend for the whole of Europe, but depending on the index, large spatial differences were found. For example, the RT index had a positive trend in the northern and central areas of Europe, but western regions returned a negative trend.

A number of previous studies showed declining rates of near-surface wind speed (termed "stilling"), which has a significant effect on the climate, such as atmospheric evaporative demand (McVicar et al., 2012; Vautard et al., 2010). In this study, a negative trend predominated in the wind indices but was not significant in the major part of the study area. On the other hand, this study showed that the indices relating to cloudiness (CC and FOD) had a negative trend, while those for radiation (ACI, SND, SSD, and SSp) were positive. Since the 1980s, there has been stabilization and recovery in surface shortwave radiation (termed "brightening") in many regions of the world (Sanchez-Lorenzo et al., 2015). There are studies explaining the brightening phenomenon due to variations in anthropogenic aerosol emissions and/or cloudiness (Wild, 2009; Sanchez-Lorenzo et al., 2015). Furthermore, Tang et al. (2012) demonstrated that summer temperatures in Europe have undergone a dramatic rise in tandem with decreased cloud cover and increased surface solar radiation. Finally, snow indices returned a negative trend across most of the territory studied. This agreed with the study by Kunkel et al. (2016) that indicated the maximum snow depth decreased in European stations from 1960 to 2015. In addition, Fontrodona Bach et al. (2018) found decreases in maximum and mean snow depth across Europe, except in the coldest climates, from 1951 onward.

4.2. Spatiotemporal Seasonal Trends of Climate Indices Throughout Europe

The overall results of trend estimation, taking into account the signal and significance trend over most of the territory studied, show clear seasonality according to the climate indices. For temperatures, the daily, maximum, and minimum mean temperatures, the number of warm nights, and the temperature of the coldest

nights increased in all seasons. Conversely, the number of cold nights and the heating degree days, a measure for the energy needed to heat buildings, decreased throughout Europe in all seasons. However, the number of warm nights and the maximum and minimum of the mean and maximum temperatures increased, while the number of cold days decreased in summer and spring and occasionally in autumn. There are abundant studies on the temperature trends in Europe; however, the comparison between them is complex, since the temporal scale (annual or seasonal) or the spatial resolution varies in the study period. Moberg and Jones (2005) highlight "the warming of winters during 1946–99 occurred in both the warm and cold tails for both Tmax and Tmin, with the largest warming in the cold tail for Tmin." Klein Tank and Können (2003) indicated an increase in temperature variability due to stagnation in the warming of the cold extremes. The increase in temperatures affects the hydrological cycle and also has serious implications for natural ecosystems, human health, and the economy, among others.

The DTR and vDTR indices (two measures of the difference between night and day records) had different signal trends depending on the season; for example, vDTR had a negative trend in winter and autumn but is positive in spring. The DTR index has a negative trend in winter but was positive in summer and spring. The DTR enables the changes in the maximum and minimum temperature to be interpreted to gain insights into the physical processes controlling surface temperatures (Collatz et al., 2000). Some authors state that there are seasonal differences in the DTR due to differences in cloudiness and insolation (Gallo et al., 1996; Lindvall & Svensson, 2015), but the reasons for large variations in time and space are unclear (Lewis & Karoly, 2013). This study shows there is a strong seasonal relationship between radiation, cloudiness and DTR. The percentages of land with a significant positive trend in DTR, CC, and SSP indices are 7%, 11%, and 4% in winter, 44%, 0%, and 55% in spring, 38%, 0%, and 64% in summer, and 13%, 2%, and 6% in autumn, respectively (Figure 6). The increase in radiation and decrease in cloudiness in summer and spring gave a positive trend in the DTR, due to the maximum temperature increase being higher than the minimum temperature (Dai et al., 1999). However, the opposite case was observed in winter with a significant positive trend across most of the land in the CC index and a small percentage in the SSp index, which led to more than two fifths of the land returning a significant negative trend in the DTR index (41%, Figure 6). Cloudiness reduces the DTR by decreasing surface solar radiation, so the minimum temperature increases more than the maximum (Dai et al., 1999). The percentage of land with a significant trend in DTR, CC, and SSP indices in autumn was very low, and it is not possible to obtain a clear signal. Nonetheless, the causes explaining the evolution of the DTR are not clear since there are other factors, such as vegetation, and its seasonal cycle that also strongly influences soil moisture, the fluxes of sensible, and latent heat, among others affecting the DTR (Zhou et al., 2007).

As previously suggested, the trend of radiation and cloudiness is linked to the temperature trend. The temporal changes in the cloud cover alter the surface-atmosphere heating distribution, due to the dominant influence of cloud on the energy balance of the Earth's climate through the cooling effect of albedo and greenhouse warming (Sun et al., 2000). In this study, the cloud/radiation indices showed a significant trend over most of the territory in spring and summer, with a positive trend in radiation indices (SSD, SSP, and ACI) and negative in cloudiness indices (CC and FOD). Trends of all-sky downward surface solar radiation from satellite-derived data over Europe (1983–2010) show a widespread increase in across most of Europe, especially in springtime (Sanchez-Lorenzo et al., 2017). The mean annual SSR series showed an increase from the mid-1980s to the early 2000s (i.e., global brightening) mainly due to anthropogenic aerosol emissions and/or cloudiness (Wild, 2009). According to Sanchez-Lorenzo et al. (2015), the recent brightening takes place primarily in spring and summer and in the eastern and central regions of Europe, as shown in the results of this study.

Cloud cover change has a strong impact on the surface shortwave radiation (Norris & Wild, 2007), atmospheric aerosols (Norris & Wild, 2007), circulation patterns (Della-Marta et al., 2007), soil moisture, and evapotranspiration (Fischer et al., 2007). In this respect, several authors (Sun et al., 2000; Tang et al., 2012) had indicated that the decreased cloud cover may have contributed to the summer warming through the effects of decrease in top of atmosphere-reflected shortwave radiation and increase in surface shortwave radiation. Other authors (Fischer et al., 2007; Hirschi et al., 2011) had suggested that a lack of sufficient amount of soil moisture has decreased latent cooling and increased the summer maximum temperature. In this study, the strong relationship between cloudiness, solar radiation, and temperature has been observed, especially in spring and summer.

The precipitation indices did not show a clear trend at seasonal scale in the study area, only the EP index (precipitation minus evapotranspiration) in summer returned a negative trend. The EP index is closely related to aridity indices, among which are ETo and CMD. The ETo index had a significant positive trend in spring and summer across most of the study area. Some authors suggest that there is increased atmospheric evaporative demand, due to a major water pressure deficit caused by higher temperatures (Vicente-Serrano et al., 2019; Wang et al., 2012), resulting in more frequent and severe droughts (Dai, 2011; Vicente-Serrano et al., 2014). This could cause biological stress, reduced soil water content, runoff generation, stream flow, and groundwater recharge (Cai & Cowan, 2008), which would impact on water management, agriculture, and aquatic ecosystems (Hisdal et al., 2001). However, the relationship between climate warming and increased atmospheric evaporative demand is the subject of scientific debate (Vicente-Serrano et al., 2019). On the other hand, the CMD index showed a north-south spatial pattern, with a positive trend in the south and a negative one in the north, especially marked in spring and summer. In this respect, Spinoni et al. (2017) indicated that drought frequency and severity showed decreasing tendencies over northern Europe, especially in winter and spring, while southern and eastern Europe showed a more significant tendency toward dryness, especially in summer and autumn, which would be explained by the evolution of the atmospheric evaporative demand (González-Hidalgo et al., 2018). In addition, Spinoni et al. (2017) pointed out that the drier conditions have recently become more prevalent over central Europe in spring, the Mediterranean area in summer, and eastern Europe in autumn. The previous results show that more severe drought, understood as the relationship between precipitation and temperature, linked to changes in the atmospheric evaporative demand, prevail in the warm season and in the south of the study area.

Otherwise, for snow, the ASD and MS indices returned a negative trend in winter and spring, and FSD and SCD only in spring. Analyzing the trend in snow data is difficult, due to the low resolution of the data against the high spatial variability of snow. Despite this, a negative trend has been observed in some snow indices, which impacts on regional water resources and reduces stream flow during the growing season when demand is heaviest, thus intensifying water scarcity in dry areas, the frequency of wildfires with those at mid-elevations burning for longer, among other issues (Schlaepfer et al., 2012).

Lastly, for wind indices, a nonsignificant negative trend was observed on an annual scale, with no large seasonal variations. A decline in the surface wind has been recorded in various parts of the world over the past few decades, but the precise cause of the stilling is uncertain; several possible reasons include increasing land surface roughness and mesoscale circulation changes (McVicar et al., 2008; Smits et al., 2005). The wind indices used in this study were estimated from the reanalysis data, and previous studies indicated that the stilling (wind slowdown) is either not reproduced or has been largely underestimated in global reanalysis products (Vautard et al., 2010; Zeng et al., 2019). Zeng et al. (2019) indicated that the wind data showed a negative trend from 1978 to 2010 and a positive trend after 2010 on a globe scale, and specifically for Europe, the stilling reversed around 2003. This study includes both trends for the 1979–2017 period, which could have affected the significance trend. The wind trend has important implications for the values and spatial distribution of the atmospheric evaporative demand, atmospheric pollution, erosion, and wind energy production, among others.

5. Conclusions

The analysis of the seasonal and annual trend of the 117 climate indices in Europe for the study period (1979–2017) shows general patterns according to the climate variable (category) of analysis.

1. The selected temperature indices show that cold days and nights had negative trends, while warm days and nights had a positive trend in most of the study territory.
2. For precipitation and aridity/continentality indices, the spatial coherence of the significant trends was low in the whole of the study area. Despite this, certain indices show spatial patterns; the RT precipitation index had a positive trend in northern and central areas of Europe, but in western regions, it was negative. Meanwhile, the CMD aridity index showed a north-south spatial pattern, with a positive trend in the south and negative in the north, especially marked in spring and summer.
3. Wind indices tended toward negative trends, but these were not significant in the major part of the study area.

4. The cloudiness indices showed a negative trend, while a positive trend was found in radiation indices over a high percentage of the study area.
5. Snow indices showed a negative trend in most of the study territory, except in the coldest regions.
6. The analysis of the seasonal trend of climate indices showed that there are large differences between seasons, reflecting the need to conduct climate studies at different time scales in order to be able to understand the causes and consequences of climate change.

This study provides a useful tool, the ECTACI viewer, to access four statistics (climatology, coefficient of variation, slope, and significant trend) from 125 climate indices for Europe at monthly, seasonal, and annual scales from 1979 to 2017. The main advantage of the ECTACI viewer is that it enables the gridded data set to be displayed and downloaded very intuitively, which makes it a valuable source of information for future studies. The four statistics obtained from the 125 climate indices at different temporal scales are available on the website http://ECTACI.csic.es/maintained by the Spanish National Research Council. The ECTACI viewer may serve as a tool in several climate services, such as validation of climate models, location of wind or solar parks, indicators for health human and tourism, and among others, besides helping to understand current climate change processes in Europe from a wide perspective.

Data Availability Statement

In our study, we use the data from the European Climate Assessment and Dataset (ECA&D) E-OBS-gridded data set v17.0 (Cornes, R. C., van der Schrier, G., van den Besselaar, E. J. M., & Jones, P. D., 2018. An Ensemble Version of the E-OBS Temperature and Precipitation Data Sets. J. Geophys. Res. Atmos. 123, 9391–9409) and the ERA5 reanalysis database (Copernicus Climate Change Service (C3S)., 2017. ERA5: Fifth generation of ECMWF atmospheric reanalyses of the global climate. Copernicus Climate Change Service Climate Data Store (CDS), date of access. https://cds.climate.copernicus.eu/cdsapp#!/home). In addition, we use the "ClimInd" package (https://cran.r-project.org/web/packages/ClimInd/index.html) within the R platform (R Core Team, R Development Team Core, 2017. A: A Language and Environment for Statistical Computing) to compute 125 climate indices. In our study, new data are generated which is deposited in a repository that belongs to the public institution Pyrenean Institute of Ecology of the Higher Council for Scientific Research (Government of Spain) http://ECTACI.csic.es/).

Acknowledgments

This work was supported by the research projects CGL2017-82216-R and CGL2017-83866-C3-1-R and PCI2019-103631, financed by the Spanish Commission of Science and Technology and FEDER; CROSSDRO project financed by the AXIS (Assessment of Cross(X) - sectorial climate Impacts and pathways for Sustainable transformation), JPI-Climate cofunded call of the European Commission and INDECIS which is part of ERA4CS, an ERA-NET initiated by JPI Climate, and funded by FORMAS (SE), DLR (DE), BMWFW (AT), IFD (DK), MINECO (ES), and ANR (FR) with cofunding by the European Union (grant 690462). Dhais Peña-Angulo received a "Juan de la Cierva" postdoctoral contract (FJCI-2017-33652 Spanish Ministry of Economy and Competitiveness, MEC).

References

Alexander, L. V., Zhang, X., Peterson, T. C., Caesar, J., Gleason, B., Tank, A. K., et al. (2006). Global observed changes in daily climate extremes of temperature and precipitation. *Journal of Geophysical Research*, *111*, D05109. https://doi.org/10.1029/2005JD006290

Amelung, B., & Viner, D. (2006). The sustainability of tourism in the Mediterranean: Exploring the future with the tourism comfort index. *Journal of Sustainable Tourism*, *14*(4), 349–366. https://doi.org/10.2167/jost549.0

Azad, A. K., Alam, M. M., & Islam, M. R. (2010). Statistical analysis of wind gust at coastal sites of Bangladesh. *International Journal of Energy Machinery*, *3*(1), 9–17.

Azorin-Molina, C., Guijarro, J. A., McVicar, T. R., Vicente-Serrano, S. M., Chen, D., Jerez, S., & Espírito-Santo, F. (2016). Trends of daily peak wind gusts in Spain and Portugal, 1961–2014. *Journal of Geophysical Research: Atmospheres*, *121*, 1059–1078. https://doi.org/10.1002/2015JD024485

Baltas, E. (2007). Spatial distribution of climatic indices in northern Greece. *Meteorological Applications: A journal of forecasting, practical applications, training techniques and modelling*, *14*(1), 69–78.

Blazejczyk, K. (2006). Climate and bioclimate of Poland. *Geographia Polonica*, *77*, 31–48.

Bröde, P., Fiala, D., Błażejczyk, K., Holmér, I., Jendritzky, G., Kampmann, B., et al. (2012). Deriving the operational procedure for the Universal Thermal Climate Index (UTCI). *International Journal of Biometeorology*, *56*(3), 481–494. https://doi.org/10.1007/s00484-011-0454-1

Cai, W., & Cowan, T. (2008). Evidence of impacts from rising temperature on inflows to the Murray–Darling Basin. *Geophysical Research Letters*, *35*, L07701. https://doi.org/10.1029/2008GL033390

Chen, D., Walther, A., Moberg, A., Jones, P., Jacobeit, J., & Lister, D. (2015). *European trend atlas of extreme temperature and precipitation records*. Dordrecht; Heidelberg; New York, NY, and London; 178: Springer.

Chiew, F. H. S., Kamaladasa, N. N., Malano, H. M., & McMahon, T. A. (1995). Penman–Monteith FAO-24 reference crop evapotranspiration and class—A pan data in Australia. *Agricultural Water Management*, *28*, 9–21.

Collatz, G. J., Bounoua, L., Los, S. O., Randall, D. A., Fung, I. Y., & Sellers, P. J. (2000). A mechanism for the influence of vegetation on the response of the diurnal temperature range to changing climate. *Geophysical Research Letters*, *27*(20), 3381–3384. https://doi.org/10.1029/1999GL010947

Copernicus Climate Change Service (C3S) (2017). ERA5: Fifth generation of ECMWF atmospheric reanalyses of the global climate. Copernicus Climate Change Service Climate Data Store (CDS), date of access. https://cds.climate.copernicus.eu/cdsapp#!/home

Cornes, R. C., van der Schrier, G., van den Besselaar, E. J. M., & Jones, P. D. (2018). An ensemble version of the E-OBS temperature and precipitation data sets. *Journal of Geophysical Research: Atmospheres*, *123*, 9391–9409. https://doi.org/10.1029/2017JD028200

Creed, I. F., Spargo, A. T., Jones, J. A., Buttle, J. M., Adams, M. B., Beall, F. D., et al. (2014). Changing forest water yields in response to climate warming: Results from long-term experimental watershed sites across North America. *Global Change Biology*, *20*(10), 3191–3208. https://doi.org/10.1111/gcb.12615

Croxford, B., Penn, A., & Hillier, B. (1996). Spatial distribution of urban pollution: Civilizing urban traffic. *Science of the Total Environment*, *189*, 3–9.

Dai, A. (2011). Drought under global warming: A review. *Wiley Interdisciplinary Reviews: Climate Change*, *2*, 45–65.

Dai, A., Trenberth, K. E., & Karl, T. R. (1999). Effects of clouds, soil moisture, precipitation, and water vapor on diurnal temperature range. *Journal of Climate*, *12*, 2451–2473.

Della-Marta, P. M., Luterbacher, J., von Weissenfluh, H., Xoplaki, E., Brunet, M., & Wanner, H. (2007). Summer heat waves over Western Europe 1880–2003, their relationship to large-scale forcings and predictability. *Climate Dynamics*, *29*, 251–275.

Di Napoli, C., Pappenberger, F., & Cloke, H. L. (2018). Assessing heat-related health risk in Europe via the Universal Thermal Climate Index (UTCI). *International Journal of Biometeorology*, *62*(7), 1155–1165.

Domínguez-Castro, F., Reig, F., Vicente-Serrano, S. M., Aguilar, E., Peña-Angulo, D., Noguera, I., et al. (2020). A multidecadal assessment of climate indices over Europe. *Scientific Data*, *7*(1), 1–7.

Easterling, D. R., Alexander, L. V., Mokssit, A., & Detemmerman, V. (2003). CCI/CLIVAR workshop to develop priority climate indices. *Bulletin of the American Meteorological Society*, *84*(10), 1403–1407.

Easterling, D. R., Evans, J. L., Groisman, P. Y., Karl, T. R., Kunkel, K. E., & Ambenje, P. (2000). Observed variability and trends in extreme climate events: A brief review. *Bulletin of the American Meteorological Society*, *81*(3), 417–426.

Falk, M. (2010). A dynamic panel data analysis of snow depth and winter tourism. *Tourism Management*, *31*(6), 912–924.

Fick, S. E., & Hijmans, R. J. (2017). WorldClim 2: New 1-km spatial resolution climate surfaces for global land areas. *International Journal of Climatology*, *37*(12), 4302–4315.

Fischer, E. M., Seneviratne, S. I., Vidale, P. L., Luthi, D., & Schar, C. (2007). Soil moisture–atmosphere interactions during the 2003 European summer heat wave. *Journal of Climate*, *20*, 5081–5099.

Fischer, G., Shah, M., N. Tubiello, F., & Van Velhuizen, H. (2005). Socio-economic and climate change impacts on agriculture: An integrated assessment, 1990–2080. *Philosophical Transactions of the Royal Society, B: Biological Sciences*, *360*(1463), 2067–2083.

Fontrodona Bach, A., Van der Schrier, G., Melsen, L. A., Klein Tank, A. M. G., & Teuling, A. J. (2018). Widespread and accelerated decrease of observed mean and extreme snow depth over Europe. *Geophysical Research Letters*, *45*, 12–312. https://doi.org/10.1029/2018GL079799

Frich, P., Alexander, L. V., Della-Marta, P. M., Gleason, B., Haylock, M., Tank, A. K., & Peterson, T. (2002). Observed coherent changes in climatic extremes during the second half of the twentieth century. *Climate Research*, *19*(3), 193–212.

Gabriels, D. (2006). Assessing the modified fournier index and the precipitation concentration index for some European countries. In J. Boardman & J. Poesen (Eds.), *Soil erosion in Europe* (Vol. 48, pp. 675–684). Wiley. https://doi.org/10.1002/0470859202.ch48

Gallo, K. P., Easterling, D. R., & Peterson, T. C. (1996). The influence of land use/land cover on climatological values of the diurnal temperature range. *Journal of Climate*, *9*, 2941–2944.

Girvetz, E. H., & Zganjar, C. (2014). Dissecting indices of aridity for assessing the impacts of global climate change. *Climatic Change*, *126*(3–4), 469–483.

Goldie, J., Alexander, L., Lewis, S. C., Sherwood, S. C., & Bambrick, H. (2019). Correction to: Changes in relative fit of human heat stress indices to cardiovascular, respiratory, and renal hospitalizations across five Australian urban populations. *International Journal of Biometeorology*, *62*(3), 423–432. https://doi.org/10.1007/s00484-017-1451-9

González-Hidalgo, J. C., Vicente-Serrano, S. M., Peña-Angulo, D., Salinas, C., Tomas-Burguera, M., & Beguería, S. (2018). High-resolution spatio-temporal analyses of drought episodes in the western Mediterranean basin (Spanish mainland, Iberian Peninsula). *Acta Geophysica*, *66*(3), 381–392.

Heim, R. R. Jr. (2015). An overview of weather and climate extremes—Products and trends. *Weather and Climate Extremes*, *10*, 1–9.

Hijmans, R. J., Cameron, S., Parra, J., Jones, P. G., Jarvis, A., & Richardson, K. (2005). WorldClim, version 1.3. University of California, Berkeley.

Hirschi, M., Seneviratne, S. I., Alexandrov, V., Boberg, F., Boroneant, C., Christensen, O. B., et al. (2011). Observational evidence for soil-moisture impact on hot extremes in southeastern Europe. *Nature Geoscience*, *4*(1), 17–21. https://doi.org/10.1038/ngeo1032

Hisdal, H., Stahl, K., Tallaksen, L. M., & Demuth, S. (2001). Have streamflow droughts in Europe become more severe or frequent? *International Journal of Climatology*, *21*(3), 317–333.

Hoegh-Guldberg, O., Jacob, D., Taylor, M., Bindi, M., Brown, S., Camilloni, I., et al. (2018). Impacts of 1.5°C global warming on natural and human systems. In *Global warming of 1.5°C: An IPCC special report on the impacts of global warming of 1.5°C above pre-industrial levels and related global greenhouse gas emission pathways, in the context of strengthening the global response to the threat of climate change, sustainable development, and efforts to eradicate poverty*. IPCC.

Hong, Y. I. N., & Ying, S. U. N. (2018). Characteristics of extreme temperature and precipitation in China in 2017 based on ETCCDI indices. *Advances in Climate Change Research*, *9*(4), 218–226.

Huang, H., Han, Y., Cao, M., Song, J., & Xiao, H. (2016). Spatial-temporal variation of aridity index of China during 1960–2013. *Advances in Meteorology*, *2016*.

IPCC (2013). In T. F. Stocker, et al. (Eds.), *Climate change 2013: The physical science basis. Contribution of Working Group I to the fifth assessment report of the intergovernmental panel on climate change* (p. 1535). United Kingdom and New York, NY, USA: Cambridge University Press.

Karl, T. R., Nicholls, N., & Ghazi, A. (1999). CLIVAR/GCOS/WMO workshop on indices and indicators for climate extremes: Workshop summary. *Climatic Change*, *42*, 3–7.

Katsanos, D., Retalis, A., Tymvios, F., & Michaelides, S. (2018). Study of extreme wet and dry periods in Cyprus using climatic indices. *Atmospheric Research*, *208*, 88–93.

Kiktev, D., Sexton, D. M. H., Alexander, L., & Folland, C. K. (2003). Comparison of modeled and observed trends in indices of daily climate extremes. *Journal of Climate*, *16*(22), 3560–3571. https://doi.org/10.1175/1520-0442(2003)016<3560:comaot>2.0.co;2

Klein Tank, A. M. G., & Können, G. P. (2003). Trends in indices of daily temperature and precipitation extremes in Europe, 1946–99. *Journal of Climate*, *16*(22), 3665–3680.

Klein Tank, A. M. G., Zwiers, F. W., & Zhang, X. (2009). Guidelines on analysis of extremes in a changing climate in support of informed decisions for adaptation, climate data and monitoring WCDMP-No 72, WMO-TD No 1500, p 5.

Koufos, G. C., Mavromatis, T., Koundouras, S., & Jones, G. V. (2018). Response of viticulture-related climatic indices and zoning to historical and future climate conditions in Greece. *International Journal of Climatology*, *38*(4), 2097–2111.

Kunkel, K. E., Robinson, D. A., Champion, S., Yin, X., Estilow, T., & Frankson, R. M. (2016). Trends and extremes in Northern Hemisphere snow characteristics. *Current Climate Change Reports*, *2*, 65–73. https://doi.org/10.1007/s40641-016-0036-8

Lewis, S. C., & Karoly, D. J. (2013). Evaluation of historical diurnal temperature range trends in CMIP5 models. *Journal of Climate*, *26*(22), 9077–9089.

Lindvall, J., & Svensson, G. (2015). The diurnal temperature range in the CMIP5 models. *Climate Dynamics*, *44*, 405–421.

Martin-Vide, J. (2004). Spatial distribution of a daily precipitation concentration index in peninsular Spain. *International Journal of Climatology*, *24*(8), 959–971.

McGregor, K. M., Marotz, G. A., & Whittemore, D. O. (1988). Ground water quality prediction using climatic indices. *Journal of the American Water Resources Association*, *24*(1), 43–48.

McVicar, T. R., Roderick, M. L., Donohue, R. J., Li, L. T., van Niel, T. G., Thomas, A., et al. (2012). Global review and synthesis of trends in observed terrestrial near-surface wind speeds: Implications for evaporation. *Journal of Hydrology*, *416*, 182–205.

McVicar, T. R., van Niel, T. G., Li, L. T., Roderick, M. L., Rayner, D. P., Ricciardulli, L., & Donohue, R. J. (2008). Wind speed climatology and trends for Australia, 1975–2006: Capturing the stilling phenomenon and comparison with near-surface reanalysis output. *Geophysical Research Letters*, *35*, L20403. https://doi.org/10.1029/2008GL035627

Moberg, A., & Jones, P. D. (2005). Trends in indices for extremes in daily temperature and precipitation in central and western Europe, 1901–99. *International Journal of Climatology: A Journal of the Royal Meteorological Society*, *25*(9), 1149–1171.

Moberg, A., Jones, P. D., Lister, D., Walther, A., Brunet, M., Jacobeit, J., et al. (2006). Indices for daily temperature and precipitation extremes in Europe analyzed for the period 1901–2000. *Journal of Geophysical Research*, *111*, D22106. https://doi.org/10.1029/2006JD007103

Moral, F. J., Paniagua, L. L., Rebollo, F. J., & García-Martín, A. (2017). Spatial analysis of the annual and seasonal aridity trends in Extremadura, southwestern Spain. *Theoretical and Applied Climatology*, *130*(3–4), 917–932.

Nicholls, S., & Amelung, B. (2008). Climate change and tourism in northwestern Europe: Impacts and adaptation. *Tourism Analysis*, *13*(1), 21–31.

Norris, J. R., & Wild, M. (2007). Trends in aerosol radiative effects over Europe inferred from observed cloud cover, solar "dimming," and solar "brightening". *Geophysical Research Letters*, *112*, D08214. https://doi.org/10.1029/2006JD007794

Osczevski, R., & Bluestein, M. (2005). The new wind chill equivalent temperature chart. *Bulletin of the American Meteorological Society*, *86*(10), 1453–1458.

Panda, D. K., Panigrahi, P., Mohanty, S., Mohanty, R. K., & Sethi, R. R. (2016). The 20th century transitions in basic and extreme monsoon rainfall indices in India: Comparison of the ETCCDI indices. *Atmospheric Research*, *181*, 220–235.

Pickering, C. (2011). Changes in demand for tourism with climate change: a case study of visitation patterns to six ski resorts in Australia. *Journal of Sustainable Tourism*, *19*(6), 767–781.

Piticar, A., Croitoru, A. E., Ciupertea, F. A., & Harpa, G. V. (2018). Recent changes in heat waves and cold waves detected based on excess heat factor and excess cold factor in Romania. *International Journal of Climatology*, *38*(4), 1777–1793.

R Core Team, R Development Team Core, (2017). R: A language and environment for statistical computing.

Rudel, E., Matzarakis, A., & Koch, E. (2007, December). Summer tourism in Austria and climate change. In MODSIM 2007 International Congress on Modelling and Simulation. Modelling and Simulation Society of Australia and New Zealand (pp. 1934–1939).

Sanchez-Lorenzo, A., Calbó, J., & Martin-Vide, J. (2008). Spatial and temporal trends in sunshine duration over Western Europe (1938–2004). *Journal of Climate*, *21*(22), 6089–6098.

Sanchez-Lorenzo, A., Enriquez-Alonso, A., Wild, M., Trentmann, J., Vicente-Serrano, S. M., Sanchez-Romero, A., et al. (2017). Trends in downward surface solar radiation from satellites and ground observations over Europe during 1983–2010. *Remote Sensing of Environment*, *189*, 108–117. https://doi.org/10.1016/j.rse.2016.11.018

Sanchez-Lorenzo, A., Wild, M., Brunetti, M., Guijarro, J. A., Hakuba, M. Z., Calbó, J., et al. (2015). Reassessment and update of long-term trends in downward surface shortwave radiation over Europe (1939–2012). *Journal of Geophysical Research: Atmospheres*, *120*, 9555–9569. https://doi.org/10.1002/2015JD023321

Schlaepfer, D. R., Lauenroth, W. K., & Bradford, J. B. (2012). Consequences of declining snow accumulation for water balance of mid-latitude dry regions. *Global Change Biology*, *18*(6), 1988–1997.

Smits, A., Klein-Tank, A. M. G., & Können, G. P. (2005). Trends in storminess over the Netherlands, 1962–2002. *International Journal of Climatology*, *25*, 1331–1344.

Spinoni, J., Naumann, G., & Vogt, J. (2017). Pan-European seasonal trends and recent changes of drought frequency and severity. *Global and Planetary Change*, *148*, 113–130.

Steadman, R. G. (1984). A universal scale of apparent temperature. *Journal of Climate and Applied Meteorology*, *23*, 1674–1687.

Stjern, C. W., Kristjánsson, J. E., & Hansen, A. W. (2009). Global dimming and global brightening—An analysis of surface radiation and cloud cover data in northern Europe. *International Journal of Climatology: A Journal of the Royal Meteorological Society*, *29*(5), 643–653.

Sun, B., Groisman, P. Y., Bradley, R. S., & Keimig, F. T. (2000). Temporal changes in the observed relationship between cloud cover and surface air temperature. *Journal of Climate*, *13*(24), 4341–4357.

Tang, Q., Leng, G., & Groisman, P. Y. (2012). European hot summers associated with a reduction of cloudiness. *Journal of Climate*, *25*(10), 3637–3644.

Toros, H. (2012). Spatio-temporal variation of daily extreme temperatures over Turkey. *International Journal of Climatology*, *32*(7), 1047–1055.

Van den Besselaar, E. J. M., Klein Tank, A. M. G., & Buishand, T. A. (2013). Trends in European precipitation extremes over 1951–2010. *International Journal of Climatology*, *33*(12), 2682–2689.

Vautard, R., Cattiaux, J., Yiou, P., Thépaut, J. N., & Ciais, P. (2010). Northern Hemisphere atmospheric stilling partly attributed to an increase in surface roughness. *Nature Geoscience*, *3*(11), 756–761.

Vicente-Serrano, S. M., Lopez-Moreno, J. I., Beguería, S., Lorenzo-Lacruz, J., Sanchez-Lorenzo, A., García-Ruiz, J. M., et al. (2014). Evidence of increasing drought severity caused by temperature rise in southern Europe. *Environmental Research Letters*, *9*(4), 044001. https://doi.org/10.1088/1748-9326/9/4/044001

Vicente-Serrano, S. M., McVicar, T. R., Miralles, D. G., Yang, Y., & Tomas-Burguera, M. (2019). Unraveling the influence of atmospheric evaporative demand on drought and its response to climate change. *Wiley Interdisciplinary Reviews: Climate Change*, e632.

Vincent, L. A., Aguilar, E., Saindou, M., Hassane, A. F., Jumaux, G., Roy, D., et al. (2011). Observed trends in indices of daily and extreme temperature and precipitation for the countries of the western Indian Ocean, 1961–2008. *Journal of Geophysical Research*, *116*, D10108. https://doi.org/10.1029/2010JD015303

Wang, K., Dickinson, R. E., & Liang, S. (2012). Global atmospheric evaporative demand over land from 1973 to 2008. *Journal of Climate*, *25*(23), 8353–8361.

Wild, M. (2009). Global dimming and brightening: A review. *Journal of Geophysical Research*, *114*, D00D16. https://doi.org/10.1029/2008JD011470

Williams, M., & Eggieston, S. (2017). Using indicators to explain our changing climate to policymakers and the public. *Bulletin WMO*, *66*(2), 201.

Winkler, A. J., Cook, J. A., Kliewer, W. M., & Lider, L. A. (1974). *General viticulture* (4th ed.). Berkeley: University of California Press.

Woodward, A., Smith, K. R., Campbell-Lendrum, D., Chadee, D. D., Honda, Y., Liu, Q., et al. (2014). Climate change and health: On the latest IPCC report. *The Lancet*, *383*(9924), 1185–1189. https://doi.org/10.1016/S0140-6736(14)60576-6

Yin, H., Donat, M. G., Alexander, L. V., & Sun, Y. (2015). Multi-dataset comparison of gridded observed temperature and precipitation extremes over China. *International Journal of Climatology*, *35*(10), 2809–2827.

Yu, G., Schwartz, Z., & Walsh, J. E. (2009). A weather-resolving index for assessing the impact of climate change on tourism related climate resources. *Climatic Change*, *95*(3–4), 551–573.

Zeng, Z., Ziegler, A. D., Searchinger, T., Yang, L., Chen, A., Ju, K., et al. (2019). A reversal in global terrestrial stilling and its implications for wind energy production. *Nature Climate Change*, *9*(12), 979–985. https://doi.org/10.1038/s41558-019-0622-6

Zhang, X., Alexander, L., Hegerl, G. C., Jones, P., Tank, A. K., Peterson, T. C., et al. (2011). Indices for monitoring changes in extremes based on daily temperature and precipitation data. *Wiley Interdisciplinary Reviews: Climate Change*, *2*(6), 851–870.

Zhou, L., Dickinson, R. E., Tian, Y., Vose, R. S., & Dai, Y. (2007). Impact of vegetation removal and soil aridation on diurnal temperature range in a semiarid region. *Proceedings of the National Academy of Sciences*, *13*, 17,937–17,942.